photonics

MDPI

Article

Numerical Study on the Soliton Mode-Locking of the Er^{3+}-Doped Fluoride Fiber Laser at ~3 μm with Nonlinear Polarization Rotation

Feijuan Zhang [1], Wenyan Yan [2], Shengnan Liang [1], Chao Tan [3] and Pinghua Tang [1,*]

[1] Hunan Key Laboratory for Micro-Nano Energy Materials and Devices, School of Physics and Optoelectronics, Xiangtan University, Xiangtan 411105, China; zhangfeijuan02@163.com (F.Z.); liangsnan@outlook.com (S.L.)

[2] School of software and communication engineering, Xiangnan University, ChenZhou 423000, China; yanwenyan333@163.com

[3] School of Information and Electrical Engineering, Hunan University of Science and Technology, Xiangtan 411201, China; chaotanhnu@163.com

* Correspondence: pinghuatang@xtu.edu.cn

Received: 16 February 2019; Accepted: 2 March 2019; Published: 6 March 2019

Abstract: Recent interest in the application of mid-infrared (mid-IR) lasers has made the generation of ~3 μm ultrafast pulses a hot topic. Recently, the generation of femtosecond-scale pulses in Er^{3+}-doped fluoride fiber lasers has been realized by nonlinear polarization rotation (NPR). However, a numerical study on these fiber lasers has not been reported yet. In this work, the output properties of the NPR passively mode-locked Er^{3+}-doped fluoride fiber ring laser in ~3 μm have been numerically investigated based on the coupled Ginzburg–Landu equation. The simulation results indicate that stable uniform solitons (0.75 nJ) with the pulse duration of femtosecond-scale can be generated from this fiber laser. This numerical investigation can provide some reference for developing the high energy femtosecond soliton fiber lasers in the mid-IR.

Keywords: Er^{3+}-doped fluoride fiber laser; mid-infrared; nonlinear polarization rotation mode-locking; ultra-short pulse

1. Introduction

Due to the potential applications in the defense, laser microsurgery, mid-infrared spectroscopy, and the pump source for longer wavelength mid-infrared or far-infrared oscillators, ultrafast pulse lasers operating in ~3 μm mid-IR wavelength band have been focused on more and more by researchers [1–3]. To date, Er^{3+}-doped fluoride fiber has been considered as a perfect gain media for ~3 μm mode-locked fiber lasers due to its broad emission wavelength band (2.71 to 2.88 μm). Moreover, its nonlinear coefficient in ~3 μm is far below those of other silica fibers (whose pulse energy is limited to ~0.1 nJ by the soliton area thorem [4]) in near-IR, which is beneficial to the production of higher energy soliton pulses from ultrafast fiber lasers [5].

Generally, ultrafast pulses can be achieved by passive mode-locking techniques. These techniques generally can be classified to two types. The first one is material saturable absorber (SA)-based mode-locking such as semiconductor saturable absorber mirrors (SESAMs) [6–8], graphene [9], and some graphene-like 2D nonlinear materials [10–16]. Nevertheless, numerous 2D material SAs are limited by the inherent deficiencies such as relatively low damage threshold and short life-time; they are hardly a guarantee of long-term operation especially when the mode-locked lasers are operated at high pulse energy. In addition, the reported pulse durations for the 2D material SAs-based mode-locking in Er^{3+}-doped fluoride fiber laser were limited to be picosecond scale due to the low modulation depth

of the material SAs in mid-IR [9,14,15]. The second one is optical Kerr-effect based mode-locking, for example, nonlinear polarization rotation (NPR) technology [17–19]. As an artificial saturable absorber, NPR technology shows the advantages of fast response time, higher damage threshold, and long-term stability at high pulse energy operation, which has been considered to be one of the most attractive approaches to achieve the stable high energy ultrafast pulse laser. Previously, researchers have realized the generation of femtosecond-scale pulses in Er^{3+}-doped fluoride fiber lasers passively mode-locked by NPR [20–22]. However, a numerical study on these fiber lasers has not been reported yet.

In this paper, we report on the numerical investigation of a NPR passively mode-locked Er^{3+}-doped fluoride fiber ring laser at ~3 μm. The simulation results indicate that this fiber laser enables the generation of stable uniform solitons up to 0.75 nJ with the pulse duration of ~500 fs.

2. Numerical Model

The schematic diagram of the NPR passively mode-locked Er^{3+}-doped fluoride fiber laser based on NPR is shown in Figure 1, which is the same cavity configuration as is involved in [20,21]. The ring cavity consists of an Er^{3+}-doped fluoride fiber, a quarter-waveplate (QWP), a half-waveplate (HWP), a polarization-dependent isolator (PD-ISO), a dichroic mirror (DM), and two focus lenses. In this cavity, the Er^{3+}-doped fluoride fiber is pumped by a 976 nm laser diode. The NPR component, consisting of a quarter-waveplate, a half-waveplate, and a polarization-dependent isolator (PD-ISO), functions as an artificial SA for mode-locking. The PD-ISO also acts as a polarizer and ensures unidirectional transmission in the ring cavity.

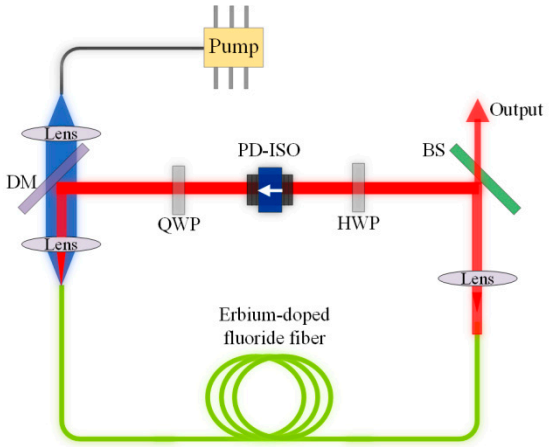

Figure 1. Schematic diagram of the passively mode-locked Er^{3+}-doped fluoride fiber laser. PD-ISO, polarization-dependent isolator; QWP, quarter waveplate; HWP, half waveplate; DM, dichroic mirror; BS, beam splitter.

We theoretically simulated the laser operation by using a pulse tracing technique. The pulse propagation in the fiber was studied on the basis of the well-known coupled Ginzburg–Landu equation, which can be written as

$$\begin{aligned} \frac{\partial u}{\partial z} &= \frac{i\Delta\beta}{2}u - \frac{i\beta_2}{2}\frac{\partial^2 u}{\partial T^2} + \frac{\beta_3}{6}\frac{\partial^3 u}{\partial T^3} + \frac{g}{2}u + i\gamma(|u|^2 + \frac{2}{3}|v|^2)u + \frac{i\gamma}{3}u^* v^2 \\ \frac{\partial v}{\partial z} &= -\frac{i\Delta\beta}{2}v - \frac{i\beta_2}{2}\frac{\partial^2 v}{\partial T^2} + \frac{\beta_3}{6}\frac{\partial^3 v}{\partial T^3} + \frac{g}{2}v + i\gamma(|v|^2 + \frac{2}{3}|u|^2)v + \frac{i\gamma}{3}v^* u^2 \end{aligned}, \quad (1)$$

where u and v are the slowly varying amplitude envelopes of the pulses along the two orthogonal polarized axes of the optical fiber, z is the propagation coordinate, T is the time scale to the pulse duration, $\Delta\beta = 2\pi/L_b$ is the wavenumber difference between the two modes, $L_b = \lambda/\Delta n$ is the beat length of cavity linear birefringence, γ is the nonlinear coefficient of the fiber, and parameters β_2 and β_3

are the second and third order dispersion coefficients of the fiber, respectively. g is the gain coefficient which can be expressed as

$$g = g(E_{\text{pulse}})(1 + T_2^2 \frac{\partial^2}{\partial t^2}), \tag{2}$$

where $T_2 = 2\pi/(ck^2\Delta\lambda_g)$, in which $\Delta\lambda_g$ is the gain bandwidth. The saturation gain $g(E_{\text{pulse}})$ can be considered as

$$g(E_{\text{pulse}}) = \frac{g_0}{1 + (E_{\text{pulse}}/E_{\text{sat}})}, \tag{3}$$

where E_{pulse} is the pulse energy, E_{sat} refers to the saturation energy, and g_0 represents the small signal gain coefficient, which is dependent on the properties of the gain fiber and pump power of the laser.

The transmission of the laser cavity has a significant impact on the mode-locking process. The light transmission through the laser cavity can be easily calculated by using the Jones matrix method [17]. The transmission T_i can be described as

$$T_i = \sin^2(\theta)\sin^2(\varphi) + \cos^2(\theta)\cos^2(\varphi) + \frac{1}{2}\sin(2\theta)\sin(2\varphi)\cos(\Delta\phi), \tag{4}$$

where θ is the angle between the fast axis of the fiber and the axis of the polarizer and ϕ is the angle between the fast axis of the fiber and the axis of the analyzer. $\Delta\varphi$ is the phase difference between the x and y polarization directions of the pulsed laser after passing through the gain fiber and the waveplates, which includes the linear polarization rotation phase bias φ_{wp} caused by the waveplates, the linear phase delay ($\Delta\varphi_{LB}$), and nonlinear phase delay ($\Delta\varphi_{NL}$) resulting from the fiber. The expressions of $\Delta\varphi$, $\Delta\varphi_{LB}$ and $\Delta\varphi_{NL}$ are as follows

$$\Delta\phi = \phi_{\text{wp}} + \Delta\phi_{\text{LB}} + \Delta\phi_{\text{NL}}, \tag{5}$$

$$\Delta\phi_{\text{LB}} = \frac{2\pi L}{\lambda}(n_x - n_y) = \frac{2\pi L}{L_b}, \tag{6}$$

$$\Delta\phi_{\text{NL}} = \frac{2\pi L(\Delta n_x - \Delta n_y)}{\lambda} = -\frac{1}{3}\gamma L(|u|^2 + |v|^2)\cos(2\theta), \tag{7}$$

where $n_x - n_y$ represents the linear birefringence, Δn_x and Δn_y are the nonlinear refractive indexes, and $(|u|^2 + |v|^2)$ is the light power in the cavity. According to Equations (4)–(7), the transmission of the fiber cavity can be calculated. The relationship between the intensity transmission T_i and the total phase delay $\Delta\varphi$ is plotted in Figure 2 for $\theta = 0.125\pi$ and $\phi = 0.625\pi$. Since NPR is equivalent to an artificial saturable absorber and the relationship between $\Delta\varphi_{NL}$ and light power is in negative correlation, the T_i increases with the light power before saturation, so we must ensure the total phase delay located at the shadow regions so as to guarantee the laser operated in the positive feedback regime.

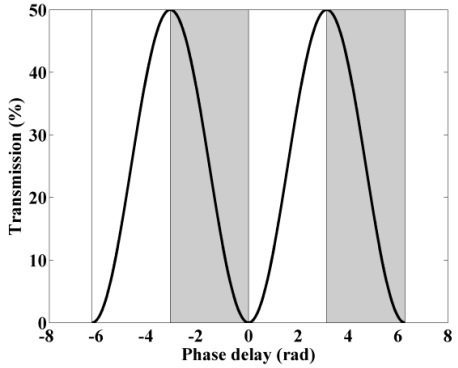

Figure 2. Cavity transmissions with respect to the total phase delay.

In order to make the simulation possibly close to the experimental situation, the parameters listed in Table 1 were used; for simplicity the effect of loss and third order dispersion of fiber are neglected. Equation (1) can be solved numerically by the symmetrized spit-step Fourier method [23] (pp. 51–55). We started a simulation with an arbitrary weak noise signal and let it circulated in the cavity. After one round trip of propagation in the cavity the calculated results were used as the input of the next round, and the procedure repeats until a stable state of optical pulse was achieved.

Table 1. Parameters used in the simulations.

Parameters	Values	References
λ	2800 nm	[21]
β_2	-86 ps^2/km	[21]
γ	0.167 W^{-1}km^{-1}	[20]
$\Delta\lambda g$	110 nm	[1]
E_{sat}	1000 pJ	-
R	0.8	-
θ	0.125π	[24]
ϕ	0.625π	[24]
φ_{wp}	1.40π	-

3. Numerical Simulation Results and Discussions

Stable soliton operation can be easily obtained by properly setting the parameters. Figure 3 shows a typical soliton mode-locking for L = 5.0 m, g_0 = 1.0 m^{-1}, and L_b = 5.0 m. We can obviously observe from Figure 3a that the mode-locked pulse is formed gradually as the round trip increase. After the 50th round trip, the pulse is further shaped into an optical soliton with uniform pulse intensity from round to round. Figure 3b is the corresponding spectra of Figure 3a. Figure 3c,d shows the output pulse and spectrum profile of the NPR mode-locked Er^{3+}-doped fluoride fiber laser in the 120th trip, respectively. From Figure 3c one can see that the pulse width and peak power are 610 fs and 1.1 kW, respectively. Obvious Kelly sidebands can be seen in the output spectrum, as depicted in Figure 3d, which means that the output pulses are typical nonlinear Schrödinger (NLS) solitons.

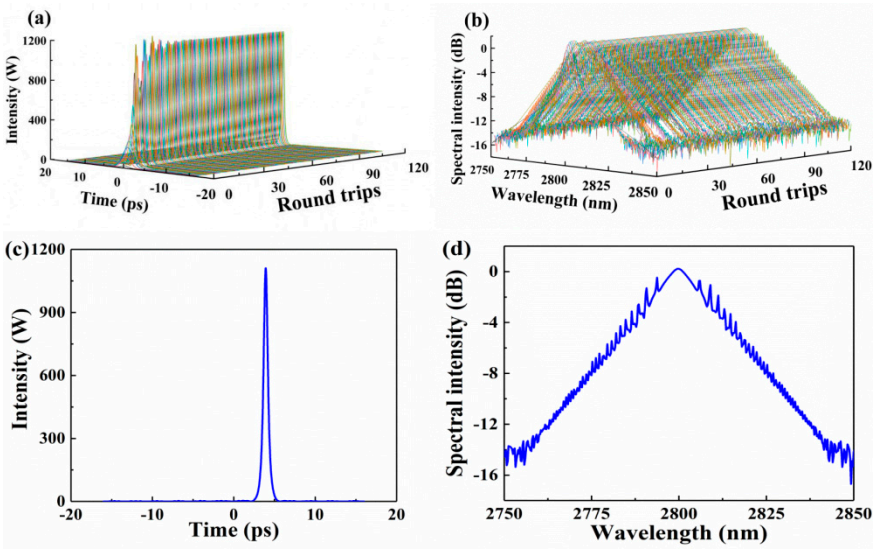

Figure 3. Pulse (**a**) and spectrum (**b**) evolution with round trips. Output pulse profile (**c**) and spectrum profile (**d**) in the 120th round trip.

NPR mode-locking requires a long cavity to acquire enough nonlinear phase shift due to the low nonlinearity of Er^{3+}-doped fluoride fiber. Thus, the influence of fiber length on the output characteristics of Er^{3+}-doped fluoride fiber laser was investigated firstly. In the simulation, the small

signal gain was set to 1.0 m^{-1}. Based on the numerical simulations, it can be found that stable uniform soliton mode-locking can be achieved for the fiber length from 3.5 to 5.0 m. Figure 4 depicts the output pulse width, 3 dB spectral bandwidth, peak power, and pulse energy with respect to the fiber length when the fiber ring laser operated in the stable soliton mode-locking state. From Figure 4a, we can see the pulse width decreases from 1520 fs at the fiber length of 3.5 m to 610 fs at the fiber length of 5.0 m, which indicates that the larger nonlinear effect originating from longer fiber length is beneficial for pulse compression. Correspondingly, with the fiber length increasing from 3.5 m to 5 m, the 3 dB spectral bandwidth increases from 7.1 nm to 17.4 nm with the corresponding time bandwidth products (TBPs) of ~0.4 for this fiber length range. The slight excess indicates that the soliton pulses are small chirped. The relationships between the peak power, pulse energy, and fiber length are shown in Figure 4b. The peak power increases from 255 W to 1.1 kW with the increase of the fiber length. Correspondingly, the pulse energy increases from 0.39 nJ to 0.68 nJ, further increasing the fiber length; stable mode-locking will disappear.

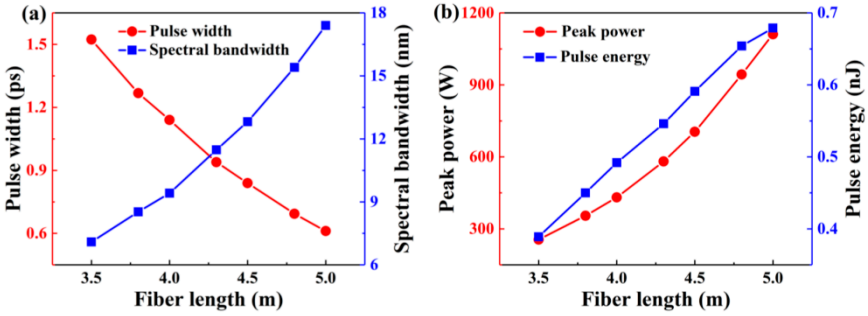

Figure 4. Output pulse characteristics of the passively mode-locked Er^{3+}-doped fluoride fiber laser. (**a**) Pulse width and 3 dB spectral bandwidth and (**b**) peak power and pulse energy as a function of fiber length.

The influence of the small signal gain on the output characteristics of the NPR mode-locked Er^{3+}-doped fluoride fiber laser was also investigated. In the simulation, the fiber length was set to 5 m. According to the simulations, stable mode-locking cannot be achieved when small signal gain below 0.8 m^{-1}. When small signal gain beyond 0.8 m^{-1}, stable uniform soliton mode-locking can be obtained as long as the small signal gain is not exceeding 1.1 m^{-1}. The output properties of the soliton pulses for the small signal gain varying from 0.8 to 1.1 m^{-1} are summarized in Figure 5. From which we can see the pulse width decreases while the peak power and pulse energy increases with the small signal gain. The narrowest pulse width of 500 fs is obtained for g_0 = 1.1 m^{-1}, with the corresponding peak power and pulse energy of 1.5 kW and 0.75 nJ, respectively. For this small signal gain range, the TBPs are calculated to be ~0.4.

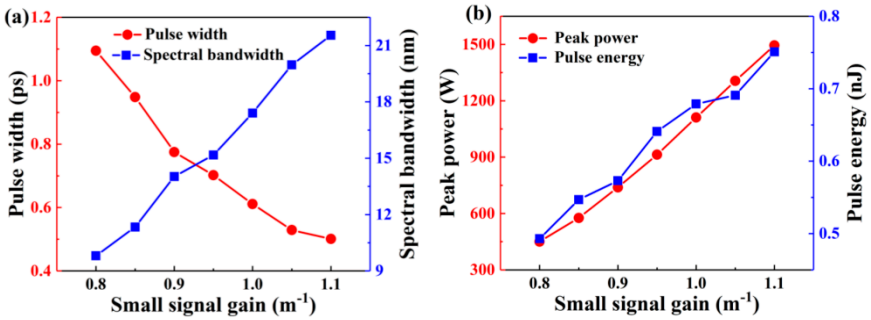

Figure 5. Output pulse characteristics of the passively mode-locked Er^{3+}-doped fluoride fiber laser. (**a**) Pulse width and 3 dB spectral bandwidth and (**b**) peak power and pulse energy as a function of small signal gain.

Figure 6a depicts the soliton pulses evolution with the increase of round trip for g_0 = 1.15 m^{-1}, from which we can see periodical slight intensity fluctuations appear on the output soliton pulses, namely, the output solitons are no longer uniform. Further increasing the small signal gain, these periodical intensity fluctuations on the output soliton pulses become more prominent, and the modulation period reduces as shown in Figure 6b, in which the small signal gain is set to 1.5 m^{-1}. In this case, narrower pulse duration of ~300 fs with higher peak power of ~2.5 kW of the solitons can be achieved. The periodical intensity fluctuations can be explained by Figure 2. Even when the laser cavity is initially biased to the positive feedback regime, it will switch to the negative feedback if the soliton peak power is overlarge. In this case, the positive feedback and negative feedback will appear periodically and, hence, the soliton pulse intensity in the laser undergoes periodical variation. There are two schemes that can suppress the periodical intensity fluctuations [25]: One is controlling the pump power below the feedback switching threshold and the other is appropriately adjusting the linear polarization bias to a position where the feedback switching threshold is higher. We would like to mention that multiple solitons will be generated by further increase of the small signal gain.

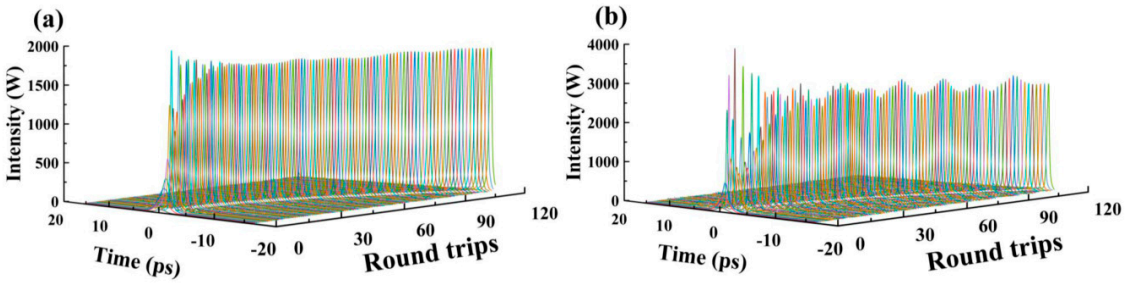

Figure 6. Pulse evolution for g_0 = 1.15 m^{-1} (**a**) and 1.5 m^{-1} (**b**) with round trips.

4. Conclusions

In conclusion, we have numerically investigated the generation of soliton pulses from an Er^{3+}-doped fluoride fiber ring laser in mid-IR near 3 μm that passively mode-locked by NPR. In the simulation, the output pulse properties of the fiber laser with various fiber lengths and small signal gains were studied. The simulation results indicate that this fiber laser enables the generation of stable uniform solitons up to 0.75 nJ (peak power of 1.5 kW) with the pulse duration of ~500 fs when the fiber length and small signal gain are set to 5 m and 1.1 m^{-1}, respectively. Further increasing the small signal gain, periodical intensity fluctuations will appear on the output soliton pulses, and a narrower pulse duration of ~300 fs with higher peak power of ~2.5 kW of the solitons can be achieved.

Author Contributions: Conceptualization, F.Z. and P.T.; Formal Analysis, F.Z., W.Y., S.L., C.T., and P.T.; Investigation, F.Z.; Methodology, F.Z.; Software, F.Z.; Supervision, P.T.; Writing—Original Draft, F.Z.; Writing—Review & Editing, F.Z., W.Y., S.L., C.T., and P.T.

Funding: This work was supported by the Hunan Provincial Natural Science Foundation of China (Grant No. 2018JJ3514), the National Natural Science Fund Foundation of China (Grant No. 61605166), the China Postdoctoral Science Foundation (Grant No. 2017M620349), and the Research Foundation of Education Bureau of Hunan Province, China (Grant No. 17C1519).

Conflicts of Interest: The authors declare no conflicts of interest.

References

1. Jackson, S.D. Towards high-power mid-infrared emission from a fibre laser. *Nat. Photon.* **2012**, *6*, 423–431. [CrossRef]
2. Zhu, X.; Peyghambarian, N. High-power ZBLAN glass fiber lasers: Review and prospect. *Adv. Opto Electron.* **2010**, *2010*, 501956. [CrossRef]
3. Shen, Y.; Huang, K.; Luan, K.; Zhu, Y.; Yu, L. 26 mJ total output from a gain-switched single-mode Er^{3+}-doped Zblan fiber laser operating at 2.8 μm. *J. Russ. Laser Res.* **2017**, *38*, 84–90. [CrossRef]

4. Wise, F.W.; Chong, A.; Renninger, W.H. High-energy femtosecond fiber lasers based on pulse propagation at normal dispersion. *Laser Photon. Rev.* **2008**, *2*, 58–73. [CrossRef]
5. Gao, C.X.; Wang, Z.Q.; Luo, H.; Zhan, L. High energy all-fiber Tm-doped femtosecond soliton laser mode-locked by nonlinear polarization rotation. *J. Lightw. Technol.* **2017**, *35*, 2988–2993. [CrossRef]
6. Tang, P.H.; Qin, Z.P.; Liu, J.; Zhao, C.J.; Xie, G.Q.; Wen, S.C.; Qian, L.J. Watt-level passively mode-locked Er^{3+}-doped ZBLAN fiber laser at 2.8 μm. *Opt. Lett.* **2015**, *40*, 4855–4858. [CrossRef] [PubMed]
7. Shen, Y.L.; Wang, Y.S.; Chen, H.W.; Luan, K.P.; Tao, M.M.; Si, J.H. Wavelength-tunable passively mode-locked mid-infrared Er^{3+}-doped ZBLAN fiber laser. *Sci. Rep.* **2017**, *7*, 14913. [CrossRef] [PubMed]
8. Hu, T.; Hudson, D.D.; Jackson, S.D. Stable, self-starting, passively mode-locked fiber ring laser of the 3 μm class. *Opt. Lett.* **2014**, *39*, 2133–2136. [CrossRef] [PubMed]
9. Zhu, G.W.; Zhu, X.S.; Wang, F.Q.; Xu, S.; Li, Y.; Guo, X.L.; Balakrishnan, K.; Norwood, R.A.; Peyghambarian, N. Graphene mode-locked fiber laser at 2.8 μm. *IEEE Photon. Technol. Lett.* **2016**, *28*, 7–10. [CrossRef]
10. Zhao, C.J.; Zhang, H.; Qi, X.; Chen, Y.; Wang, Z.T.; Wen, S.C.; Tang, D.Y. Ultra-short pulse generation by a topological insulator based saturable absorber. *Appl. Phys. Lett.* **2012**, *101*, 201106. [CrossRef]
11. Chen, Y.; Wu, M.; Tang, P.H.; Chen, S.Q.; Du, J.; Jiang, G.B.; Li, Y.; Zhao, C.J.; Zhang, H.; Wen, S.C. The formation of various multi-soliton patterns and noise-like pulse in a fiber laser passively mode-locked by a topological insulator based saturable absorber. *Laser Phys. Lett.* **2014**, *11*, 055101. [CrossRef]
12. Woodward, R.I.; Howe, R.C.T.; Hu, G.; Torrisi, F.; Zhang, M.; Hasan, T.; Kelleher, J.R. Few-layer MoS_2 saturable absorbers for short-pulse laser technology: Current status and future perspectives. *Photon. Res.* **2015**, *3*, A30–A42. [CrossRef]
13. Sotor, J.; Sobon, G.; Macherzynski, W.; Paletko, P.; Abramski, K.M. Black phosphorus saturable absorber for ultrashort pulse generation. *Appl. Phys. Lett.* **2015**, *107*, 051108. [CrossRef]
14. Li, J.F.; Luo, H.Y.; Zhai, B.; Lu, R.G.; Guo, Z.N.; Zhang, H.; Liu, Y. Black phosphorus: A two-dimension saturable absorption material for mid-infrared Q-switched and mode-locked fiber lasers. *Sci. Rep.* **2016**, *6*, 30361. [CrossRef] [PubMed]
15. Qin, Z.P.; Xie, G.Q.; Zhao, C.J.; Wen, S.C.; Yuan, P.; Qian, L.J. Mid-infrared mode-locked pulse generation with multilayer black phosphorus as saturable absorber. *Opt. Lett.* **2016**, *41*, 56–59. [CrossRef] [PubMed]
16. Ge, Y.Q.; Zhu, Z.F.; Xu, Y.H.; Chen, Y.X.; Chen, S.; Liang, Z.M.; Song, Y.F.; Zou, Y.S.; Zeng, H.B.; Xu, S.X.; et al. Broadband nonlinear photoresponse of 2D TiS_2 for ultrashort pulse generation and all-optical thresholding devices. *Adv. Opt. Mater.* **2018**, *6*, 1701166. [CrossRef]
17. Lyu, Y.; Li, J.F.; Hu, Y.X.; Wang, Y.Z.; Wei, C.; Liu, Y. Theoretical comparison of NPR and hybrid mode-locked soliton thulium-doped fiber lasers. *IEEE Photon. J.* **2017**, *9*, 1–11. [CrossRef]
18. Zhao, L.M.; Tang, D.Y.; Wu, X.; Zhang, H. Dissipative soliton generation in Yb-fiber laser with an invisible intracavity bandpass filter. *Opt. Lett.* **2010**, *35*, 2756–2758. [CrossRef] [PubMed]
19. Nikodem, M.P.; Budnicki, A.; Tomczyk, G.; Abramski, K.M. Investigation of passively mode-locked erbium doped fiber ring laser due to nonlinear polarization rotation. *Opto-Electron. Rev.* **2008**, *16*, 194–198. [CrossRef]
20. Hu, T.; Jackson, S.D.; Hudson, D.D. Ultrafast pulses from a mid-infrared fiber laser. *Opt. Lett.* **2015**, *40*, 4226–4228. [CrossRef] [PubMed]
21. Duval, S.; Bernier, M.; Fortin, V.; Genest, J.; Piché, M.; Vallée, R. Femtosecond fiber lasers reach the mid-infrared. *Optica* **2015**, *2*, 623–625. [CrossRef]
22. Antipov, S.; Hudson, D.D.; Fuerbach, A.; Jackson, S.D. High-power mid-infrared femtosecond fiber laser in the water vapor transmission window. *Optica* **2016**, *3*, 1373–1376. [CrossRef]
23. Agrawal, G.P. *Nonlinear Fiber Optics*, 3rd ed.; Academic Press: San Diego, CA, USA, 2001; pp. 51–55.
24. Man, W.S.; Tam, H.Y.; Demokan, M.S.; Wai, P.K.A.; Tang, D.Y. Mechanism of intrinsic wavelength tuning and sideband asymmetry in a passively mode-locked soliton fiber ring laser. *J. Opt. Soc. Am. B* **2000**, *17*, 28–33. [CrossRef]
25. Zhao, B.; Tang, D.Y.; Zhao, L.M.; Shum, P.; Tam, H.Y. Pulse-train nonuniformity in a fiber soliton ring laser mode-locked by using the nonlinear polarization rotation technique. *Phys. Rev. A* **2004**, *69*, 043808. [CrossRef]